Journal of Power Sources 182 (2008) 298–306

Contents lists available at ScienceDirect

Journal of Power Sources

journal homepage: www.elsevier.com/locate/jpowsour

Autothermal reforming of gasoline for fuel cell applications: Controller design and analysis

Yongyou Hu [a], Donald J. Chmielewski [a,*], Dennis Papadias [b]

[a] Center for Electrochemical Science and Engineering, Department of Chemical and Biological Engineering, Illinois Institute of Technology, 10 W. 33rd Street, Suite 127, Chicago, IL 60616, USA
[b] Chemical Engineering Division, Argonne National Laboratory, 9700 South Cass Avenue, Argonne, IL 60439, USA

ARTICLE INFO

Article history:
Received 10 January 2008
Received in revised form 15 March 2008
Accepted 18 March 2008
Available online 25 March 2008

Keywords:
Fuel cells
Autothermal reforming
Feedback control
Feed-forward control

ABSTRACT

In this work, we address the control system options available to an autothermal reforming (ATR) reactor. The targeted application is within an on-board fuel processor for a hydrogen-fed low-temperature fuel cell. The feedback controller employs air feed rate as the manipulated variable and a measurement of catalyst temperature as the control variable. Disturbances include significant fluctuations in the measured temperature as well as large throughput changes, owning to the on-board application. Our investigation includes an analysis of a simple feedback configuration as well as feed-forward control structure. It is concluded that the feedback only method is insufficient for the unique challenges associated with on-board operation, which include fast start-up and quick load changes. While the feed-forward configuration improves performance, we found a fair amount of sensitivity with respect to model mismatch. The general conclusion is that some form of advanced control will be needed to meet the stringent performance requirements of the on-board fuel processor application.

1. Introduction

A fundamental question concerning the operation of an autothermal reforming (ATR) reactor within an on-board fuel processor application is, if classic methods can be used to control the reactor. Although the highly nonlinear nature of the reactor suggests the need for an advanced controller, this hypothesis has never been fully investigated. The objective of the current study is to determine if classic control methods are sufficient. Clearly, this is a prerequisite step before investing the significant effort required to develop an advanced controller.

The paper is organized as follows. The next section will provide background information concerning the on-board fuel processor application, as well as a literature review. Then, we perform an open-loop modeling study intended to provide initial tuning parameters for the subsequent controller design. In Section 4, we analyze closed-loop performance of the classic feedback controller in the face of changes in hydrogen demand. In general, these changes are the result of reactor start-up or a change in the amount of hydrogen requested by the fuel cell (i.e., a power load change). In Section 5, we will focus on the performance of feed-forward plus feedback control for start-up and large load changes. The analysis of robustness will also be conducted in this section.

2. Background

One of the many challenges to the development of a fuel cell system for transportation applications is that of a fuel delivery system. While on-board hydrogen storage is desired, this option is frustrated by the insufficient energy density of existing storage technologies as well as the lack of a hydrogen distribution infrastructure. The alternative is to install an on-board hydrogen generation unit to convert high energy density hydrocarbon fuels. Unfortunately, this unit will add substantially to the volume, weight, and complexity of the overall system. Additionally, the response time of the overall system will be degraded by that of the fuel processor.

The current effort is just one component of a larger project aimed at identifying the start-up capabilities of a fuel processing unit [1]. This project (titled the Feasibility of Acceptable Start-Time Experimental Reformer [FASTER] project) was charged with constructing a 10-kWe system and showing that it could be started in less than 60 s. Additional criteria of the project included size, weight, and efficiency parameters as well as a maximum allocation of reactor heating energy available for the start-up phase. A flow diagram of the constructed FASTER process is depicted in Fig. 1. At

* Corresponding author. Tel.: +1 312 567 3537; fax: +1 312 567 8874.
E-mail address: chmielewski@iit.edu (D.J. Chmielewski).

0378-7753/$ – see front matter © 2008 Elsevier B.V. All rights reserved.
doi:10.1016/j.jpowsour.2008.03.041

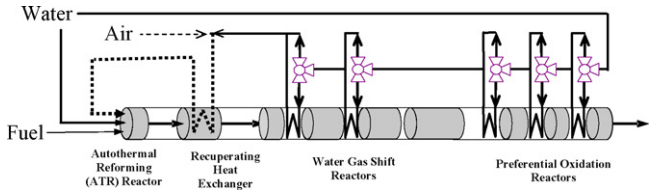

Fig. 1. Flow diagram of the FASTER fuel processor.

the heart of the process, we find the autothermal reforming (ATR) reactor. Within this reactor, it is sufficient to assume that three non-elementary reactions take place [2]:

Total oxidation:

$$C_mH_n + \left(m + \left(\frac{n}{4}\right)\right) O_2 \rightarrow mCO_2 + \frac{n}{2}H_2O \quad (1)$$

Steam reforming:

$$C_mH_n + mH_2O \rightarrow mCO + \left(m + \left(\frac{n}{2}\right)\right) H_2 \quad (2)$$

Water–gas shift:

$$CO + H_2O \leftrightarrow CO_2 + H_2 \quad (3)$$

During start-up of the ATR reactor, there are two primary goals. The first is to generate sufficient heat such that the reactor will reach the desired operating temperature as soon as possible. The second is to achieve a sufficiently low CO concentration in the reformate stream. To achieve the first goal, the ATR is started in catalytic partial oxidation (CPOX) mode (that is, using a feed of only fuel and air). To achieve the second goal, steam is added to the feed so as to drive the equilibrium-limited shift reaction toward greater conversion of CO. This second set of conditions is denoted as the ATR mode. An additional consequence of steam injection is a significant drop in reactor temperature that threatens to extinguish the reaction. In response to this temperature dip, one should simultaneously increase air flow rate. However, this increase should be such that the reactor temperature does not exceed operational limits, and possibly damage the catalyst. Post start-up operational objectives are similar. Specifically, in the face of changing hydrogen demands the controller must continuously satisfy operational bounds with respect to reactor temperatures.

From a control engineering perspective, the open-loop plant is the ATR reactor depicted in Fig. 2. The input and output signals of this plant will be discussed next. The set of inputs includes the inlet flow rates of air, steam and fuel as well as the temperature of this inlet gas stream. While a measurement of each is expected, the degree to which each can be manipulated varies. For example, the inlet temperature, in principle, can be influenced by the heating rods located in front of the catalyst surface, see Fig. 2. However, toward the objective of electrical efficiency, these rods will be turned off once the combustion reaction has been ignited. It should also be noted that inlet temperature will depend heavily on the state of the recuperating heat exchanger on the upstream air flow. Regarding the inlet of fuel and steam, Figs. 1 and 2 indicate these to be from a variety of sources. Specifically, steam will come from a dedicated vaporizer (not depicted) during the start-up phase, and subsequently from the exit of heat exchangers used to cool downstream units. As an alternative to the low efficiency of a vaporizer, a nozzle could be applied to generate a fine mist of liquid droplets at the reactor inlet. Similarly, the fuel inlet could be a dry vapor stream or a nozzle generated mist, with the possibility of switching between the two. Clearly, each of these options and the thermal state of the hardware used to generate these streams will influence the reactor conditions. However, rather than attempt to model these ancillary units, we will lump them all into the notion of inlet temperature as disturbance. If we further assume that each stream is fully vaporized (i.e., exclude the nozzle option), then the inlet temperature disturbance, as we have defined it, is measurable and fairly slow to change. Concerning measurable outputs, the set of outputs is limited to four thermocouples on the solid catalyst support at various axial locations, see Fig. 2. These measurements are at the following locations: 0.08 cm, 0.7 cm, 1.9 cm and 3.1 cm (indicated by T_1, T_2, T_3 and T_4, respectively). In the analysis and model validation of [2], exit concentration of CO and H_2 were utilized. However, in a production scale system the availability of these measurements is unlikely and thus will be ignored in the current study.

In the literature, we find a number of experimental and simulation-based studies concerning the start-up and dynamic performance of on-board CPOX and ATR reactors [1–4]. However, application of this knowledge to the design of controllers for these reactors is just beginning to appear. In El-Sharkh et al. [5], a methanol reformer unit is modeled by a second-order transfer function. The exit flow of hydrogen is then PI-controlled through manipulation of the methanol feed. In Gorgun et al. [6], an observer-based method is applied to a CPOX reactor to estimate the species content of the exit stream. Although a specific control structure

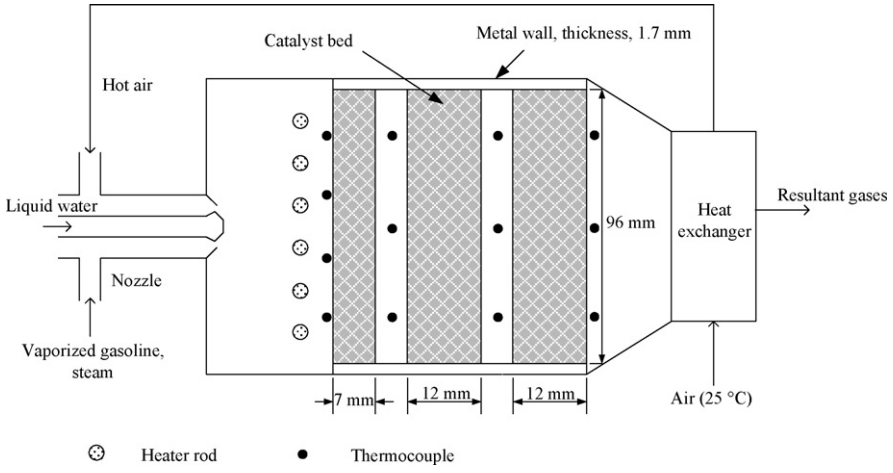

Fig. 2. Schematic of the ATR reactor.

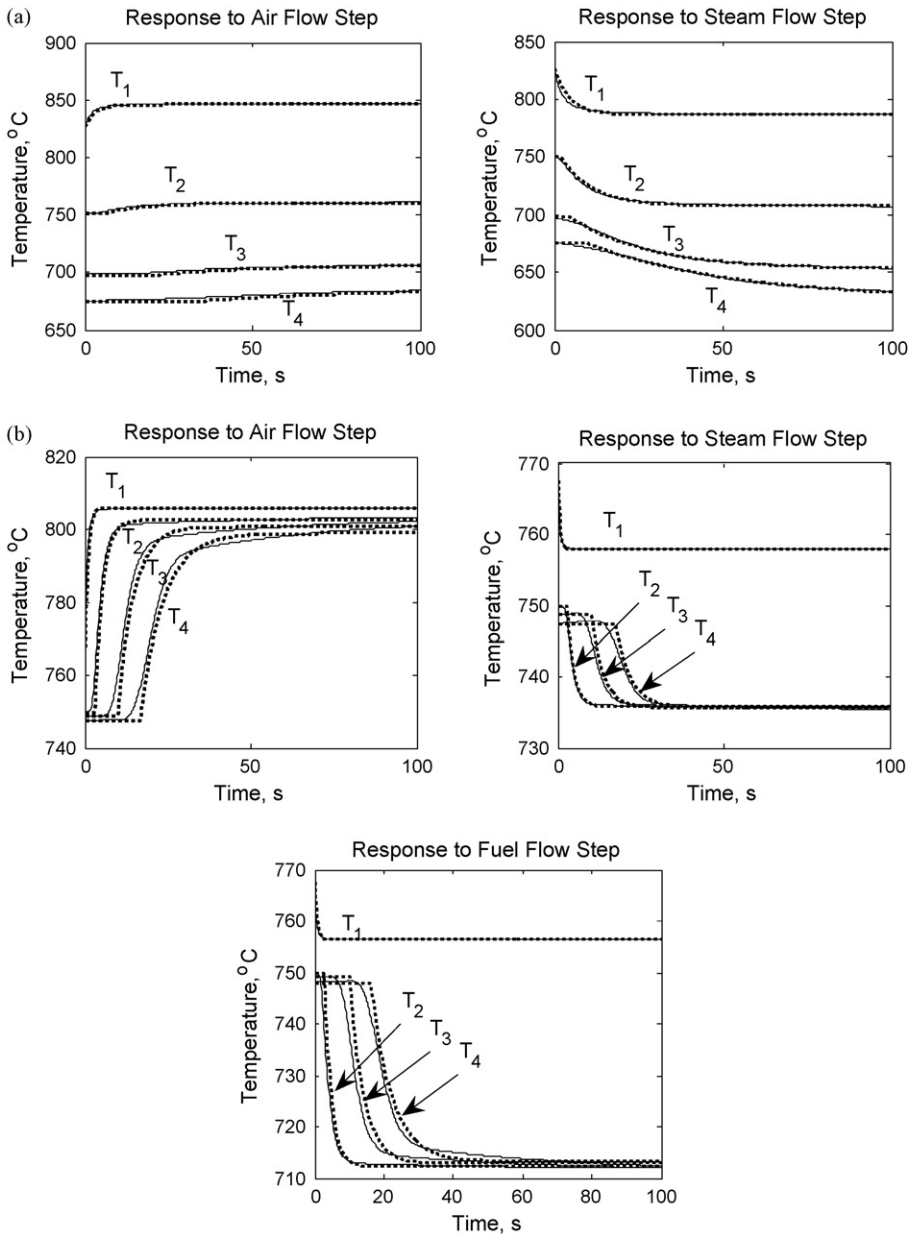

Fig. 3. (a) Comparison of 1D (solid line) and 0D (dotted line) models: CPOX mode. (b) Comparison of 1D (solid line) and 0D (dotted line) models: ATR mode.

is not discussed, the proposed CPOX model (a lumped-parameter, nonlinear, state-space form with respect to molar holdups and catalyst temperature) suggested that fuel and air feed rates will be used as manipulated variables. The collaborative effort between the University of Michigan and the United Technologies Research Center has produced a number of papers on the control of methane-fed CPOX reactors (see [7–9]). In these efforts, lumped-parameter nonlinear models with respect to molar flow rates and catalyst temperature were proposed for the CPOX reactor. These were then combined with similar models for auxiliary units and the fuel cell. The proposed scheme aimed to regulate CPOX temperature as well as fuel cell hydrogen mole fraction through manipulation of the inlet methane and air flow rates. The current drawn from the fuel cell was the assumed disturbance. The proposed control structure employed a feedback element as well as a feed-forward unit. Using relative gain array analysis (on a linearized version of the model), decentralized PI pairings were determined (identified as air flow to CPOX temperature and fuel flow to hydrogen mole fraction). Additionally, an observer-based linear quadratic regulator was proposed. Simulations with respect to the nonlinear model indicated that both controllers would perform reasonably well. Regarding the control of ATR reactors, we could not find any citations other than passing references in two U.S. Patents [10,11].

Table 1
Nominal operating condition for different modes

Mode	CPOX	ATR
Fuel flow rate (g min^{-1})	22.9	22.9
Air flow rate (dm^3 min^{-1})	24.3	82.8
Steam flow rate (g min^{-1})	0	162.8
Inlet temperature (°C)	250	450
Hydrogen yield (mol min^{-1})	0.3	3.0

Table 2
FOPDT model parameters for CPOX mode

Output	$T_i/F_{Air,in}$			$T_i/F_{Steam,in}$		
T_i	K_i	τ_i	θ_i	K_i	τ_i	θ_i
$i=1$	7.32	3.1	0	−13.34	4.38	0
$i=2$	3.54	11.3	5.6	−14.44	9.4	1.8
$i=3$	3.35	28.7	20	−14.84	23.2	5
$i=4$	4.47	54	33.3	−16.2	44	10

Table 3
FOPDT model parameters for ATR mode

Output	$T_i/F_{Air,in}$			$T_i/F_{Steam,in}$			$T_i/F_{Fuel,in}$		
T_i	K_i	τ_i	θ_i	K_i	τ_i	θ_i	K_i	τ_i	θ_i
$i=1$	4.63	0.9	0	−0.59	0.44	0.1	−4.9	0.74	0
$i=2$	6.38	2.34	2.9	−0.86	2.0	2.7	−16.4	2.0	2.8
$i=3$	6.28	4.7	9.9	−0.8	3.5	10.2	−15.8	4.0	10.1
$i=4$	6.22	7.0	16.5	−0.72	4.6	17.2	−15.1	6.0	16.2

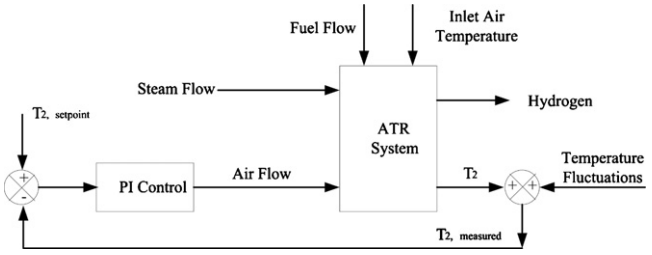

Fig. 4. Feedback control structure.

3. Process characterization

In [2], a dynamic axially dependent model of the ATR reactor was developed. In the current study of controller performance, we utilize a revised nonlinear model where the thermal model was converted from partial differential equations to ordinary differential equations. The simulations resulting from these two models are nearly identical (see ROM1 of [12] for details). The transfer functions used during controller design were identified from step responses generated by the revised nonlinear model.

The possible control variables (CVs) are solid temperatures and the possible manipulated variables (MVs) include the inlet flow rates of air, fuel, and steam. Fig. 3 illustrates a portion of the simulated data along with the output of the fit 0-D models at nominal CPOX and ATR operating conditions, listed in Table 1. The step inputs applied in Fig. 3a were +10% of the nominal air flow rate and +3 g min^{-1} of steam flow rate. For Fig. 3b the inputs were +10% of the nominal values.

The simulated data was then fit to first-order plus dead time (FOPDT) transfer function models of the form:

$$\frac{T_i}{F_{Air,in}} = \frac{K_i e^{-\theta_i s}}{\tau_i s + 1}, \quad \frac{T_i}{F_{Steam,in}} = \frac{K_i e^{-\theta_i s}}{\tau_i s + 1} \quad \text{and} \quad \frac{T_i}{F_{Fuel,in}} = \frac{K_i e^{-\theta_i s}}{\tau_i s + 1} \quad (4)$$

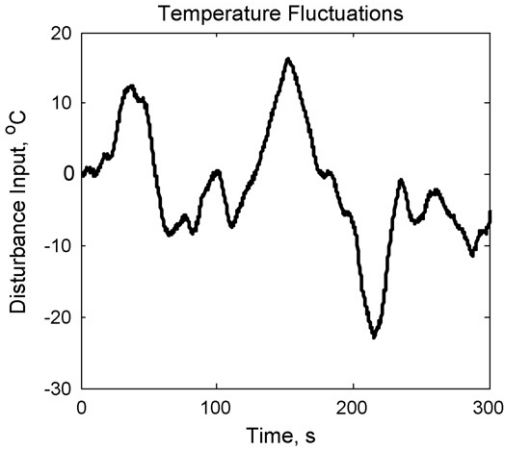

Fig. 5. Expected disturbances due to temperature fluctuations.

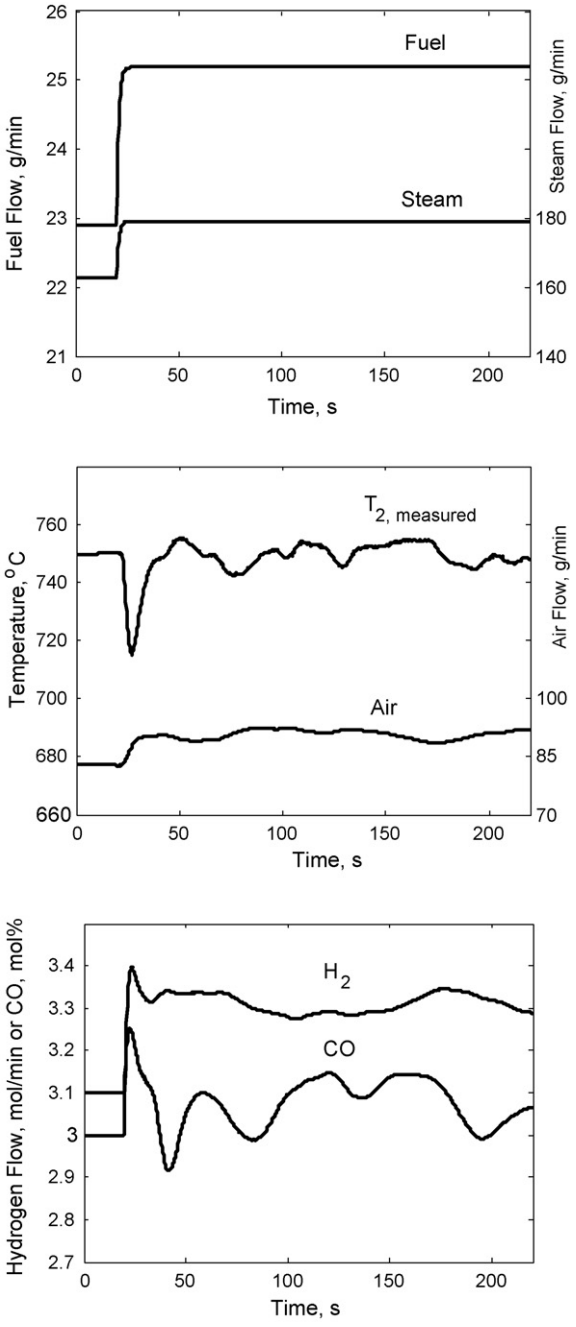

Fig. 6. Input and output responses to a load change (+10%) with feedback control.

The identified parameters K_i, τ_i and θ_i for the CPOX and ATR modes can be found in Tables 2 and 3. The parameters show significant variation due to the strong nonlinear characteristics of ATR reactor.

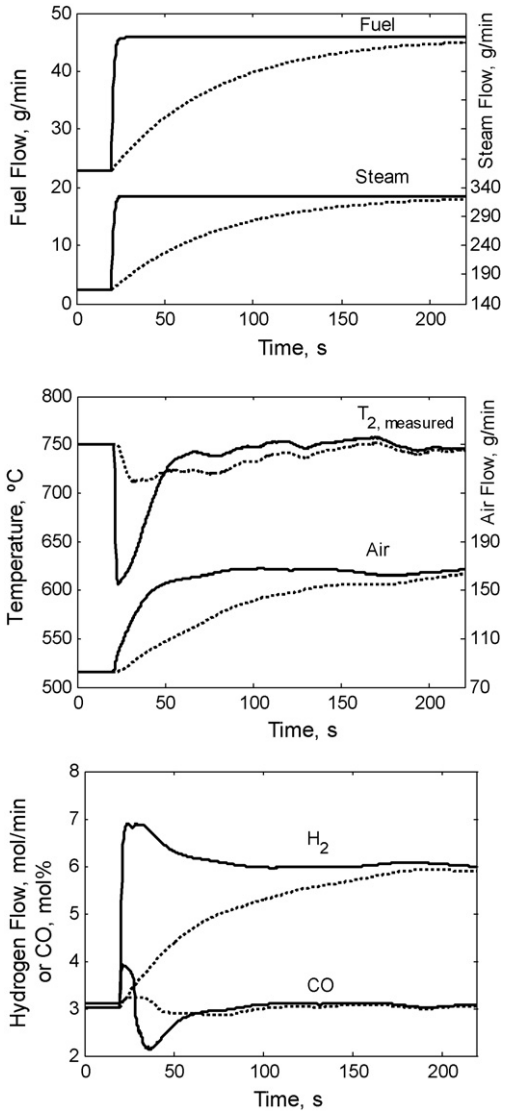

Fig. 7. Input and output responses to a load change (+100%) with feedback control (solid line: $\tau_s = 1$ s; dotted line: $\tau_s = 60$ s).

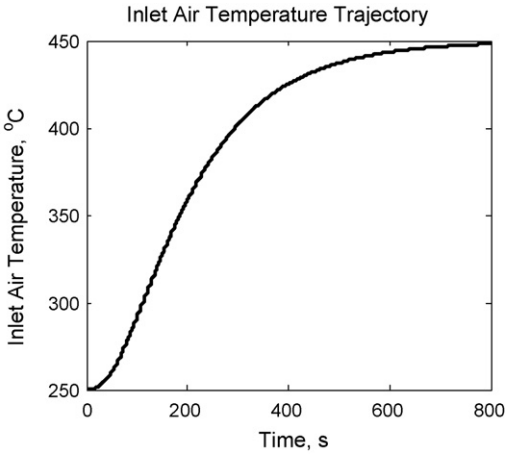

Fig. 8. Expected trajectory of the inlet air temperature for start-up.

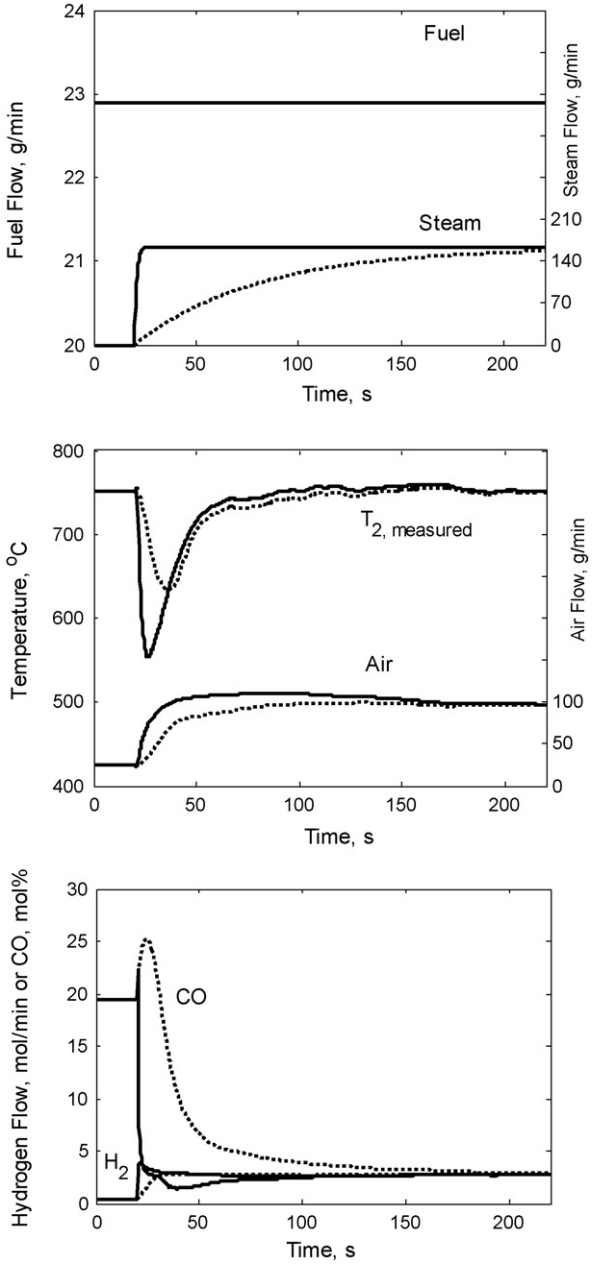

Fig. 9. Input and output responses to start-up with feedback control (solid line: $\tau_s = 1$ s; dotted line: $\tau_s = 60$ s).

It should also be noted that these model parameters are only valid for the specific ATR size and geometry considered in this study.

4. Classic feedback control

The feedback structure used in this section is depicted in Fig. 4. Here we see that the MV is selected to be the inlet flow rate of air, which will increase all reactor temperatures if increased (as indicated by the parameter values of Tables 2 and 3). Furthermore, the figure indicates that the selected CV is T_2, which is the measured temperature with smallest time delay (the time delay of T_1 is smaller, but T_1 is not expected to be measurable in production scale systems).

From Fig. 4, we additionally see two types of disturbances. The first is due to changes in the inlet air temperature. The second dis-

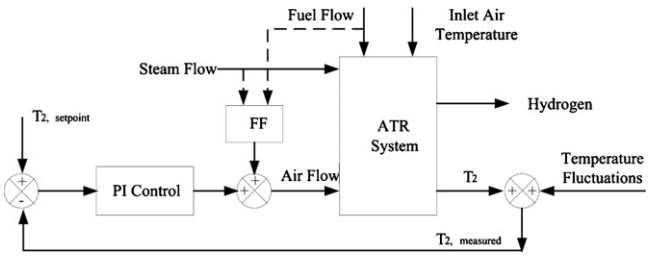

Fig. 10. Feed-forward control structure.

turbance represents fluctuations in the reactor temperature due to radial nonuniformities. These we model as Gaussian white noise filtered through a linear system with transfer function $33/(7.5s+1)(5s+1)(2.5s+1)$. This filtering allows for the capture of intermediate frequency disturbances, which are distinct from the mostly high frequency content of the sensor noise (see Fig. 5). Compared with the temperature fluctuations, the sensor noise is much smaller and thus neglected.

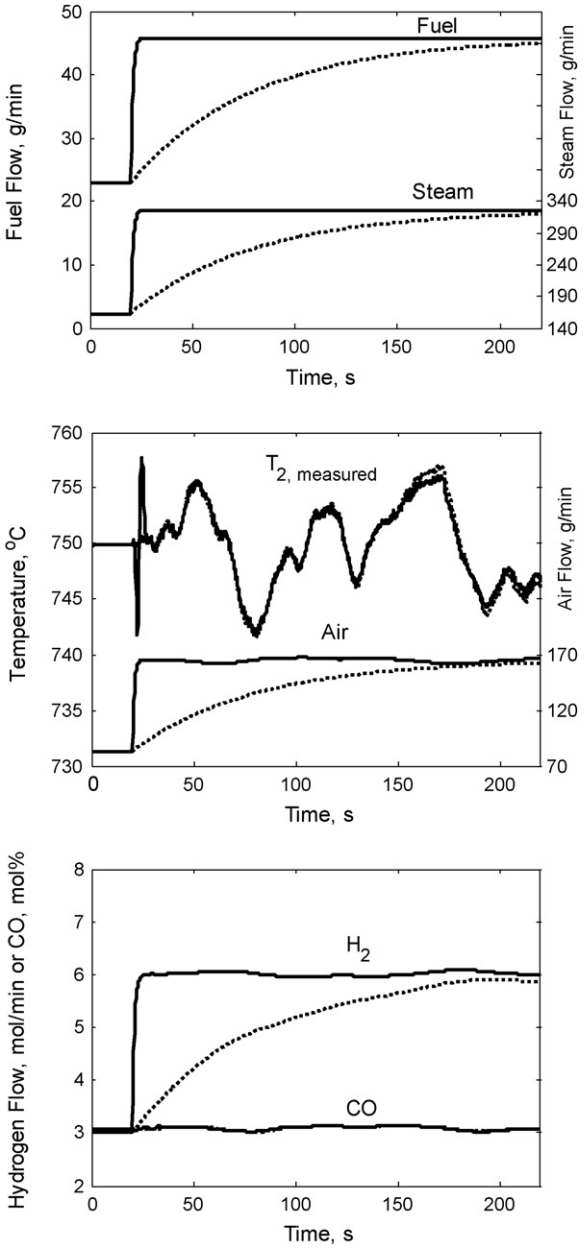

Fig. 11. Input and output responses to a load change (+100%) with feed-forward control (solid line: $\tau_s = 1$ s; dotted line: $\tau_s = 60$ s).

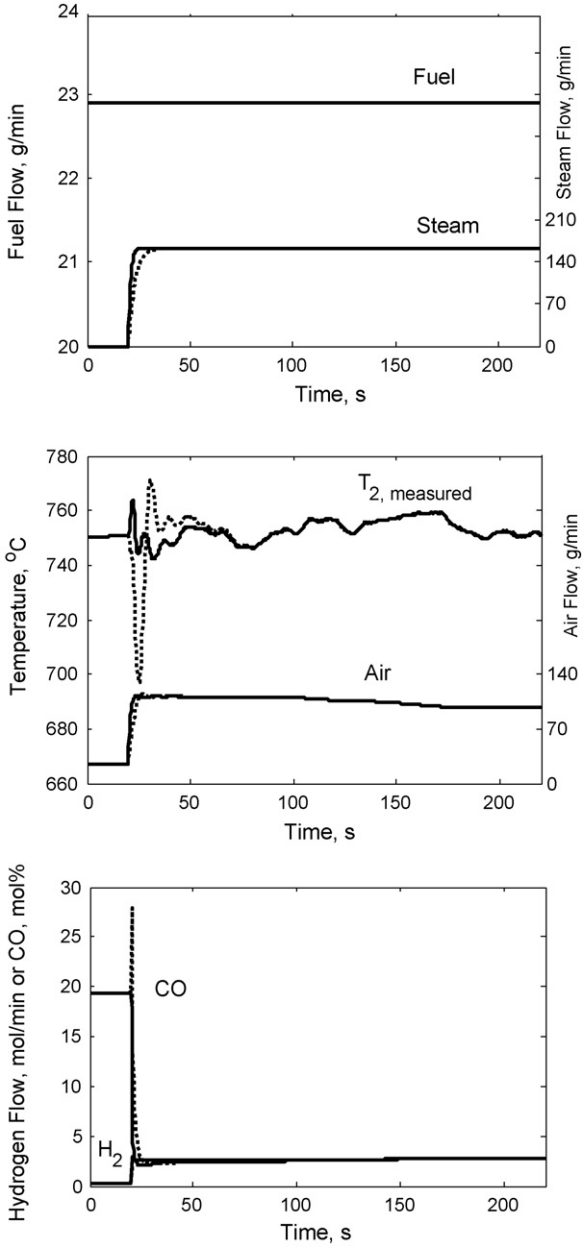

Fig. 12. Input and output responses to start-up with feed-forward control (solid line: $\tau_s = 1$ s; dotted line: $\tau_s = 3$ s).

The tuning values for the PI controller were selected as [13]:

$$K_c = \frac{\tau}{\tau_c + \theta}\frac{1}{K} \quad \text{and} \quad \tau_i = \tau \tag{5}$$

where $K = K_2$, $\tau = \tau_2$ and $\tau_c = \theta_2$ were taken from Tables 2 and 3 depending on the operating mode.

4.1. Feedback control during nominal operation

During nominal operation the reactor is operated in ATR mode, and will frequently face load changes due to changes in hydrogen demand from the fuel cell. Fig. 6 shows the closed-loop response of

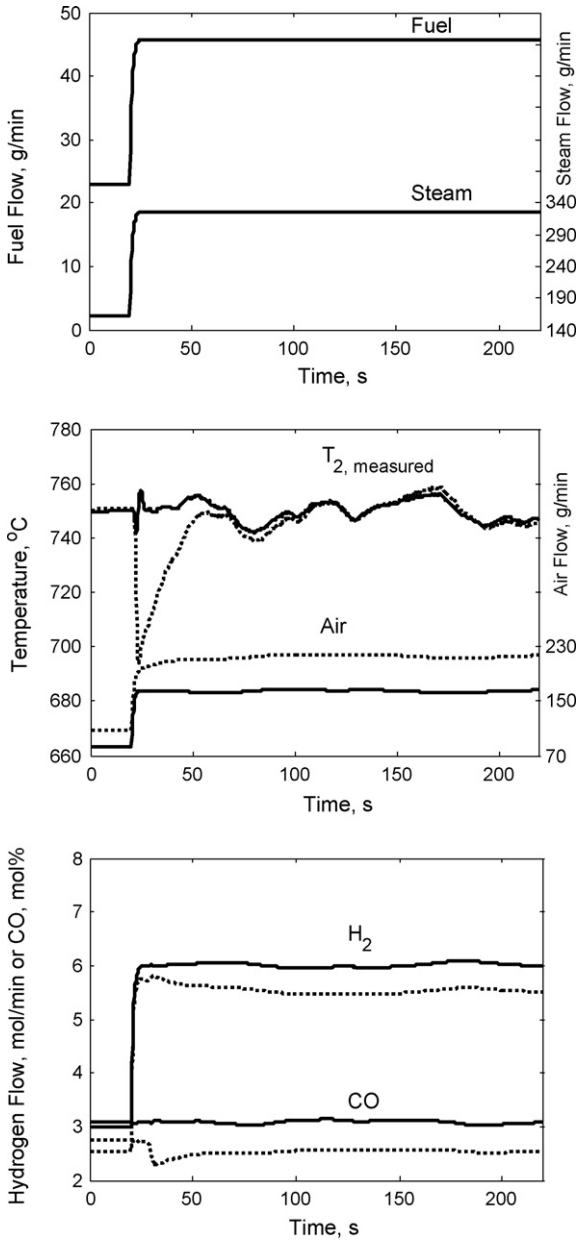

Fig. 13. Input and output responses to a load change with feed-forward control for different gasolines (solid line: $C_{7.3}H_{14.28}$; dotted line: C_8H_{18}).

the system due to a load change of +10% of the nominal hydrogen production rate, 0.3 mol min^{-1}. This load change was initiated by changing the fuel and steam flow rates. In this paper, we assume that the fuel and steam flows are determined by some external entity, either a higher level controller or the system operator. In either case, it is the responsibility of the controller of Fig. 4 to respond to these external disturbances. In an effort to parameterize the intent of this external entity, we have prescribed the fuel and steam flow trajectories as first-order step responses with a time constant τ_s. This parameter will allow us to choose the speed at which the change is desired. In the scenario of Fig. 6, $\tau_s = 1$ s and the inlet air temperature was 450 °C.

As shown in Fig. 6 (middle), the load change transition causes an initial temperature dip (~32 °C) and then the reactor temperature is well controlled to within ±10 °C in the face of the temperature fluctuation disturbance. The hydrogen demand, Fig. 6 (bottom), responds to the load change very quickly (within 5 s) and the concentration of CO is also well controlled. While very good performance is observed in the face of a small load change, this level of performance is not observed in the face of larger load changes, e.g., +100%. In Fig. 7, the hydrogen demand is changed from 3 to 6 mol min^{-1}, with the same feedback controller. However, a substantial drop in reactor temperature (~150 °C) is observed for the fast fuel and steam injection, $\tau_s = 1$ s (see the solid lines of Fig. 7) and the reactor may extinguish ($T_2 < 700$ °C). The temperature drop can be reduced by slowing the fuel and steam injection rate, $\tau_s = 60$ s (see the dotted lines of Fig. 7). However, the all important hydrogen transition will take much longer (around 100 s) as shown in Fig. 7 (bottom).

4.2. Feedback control during start-up

The most challenging aspect of reactor start-up is the transition from CPOX to ATR mode. This is achieved by fixing the fuel flow

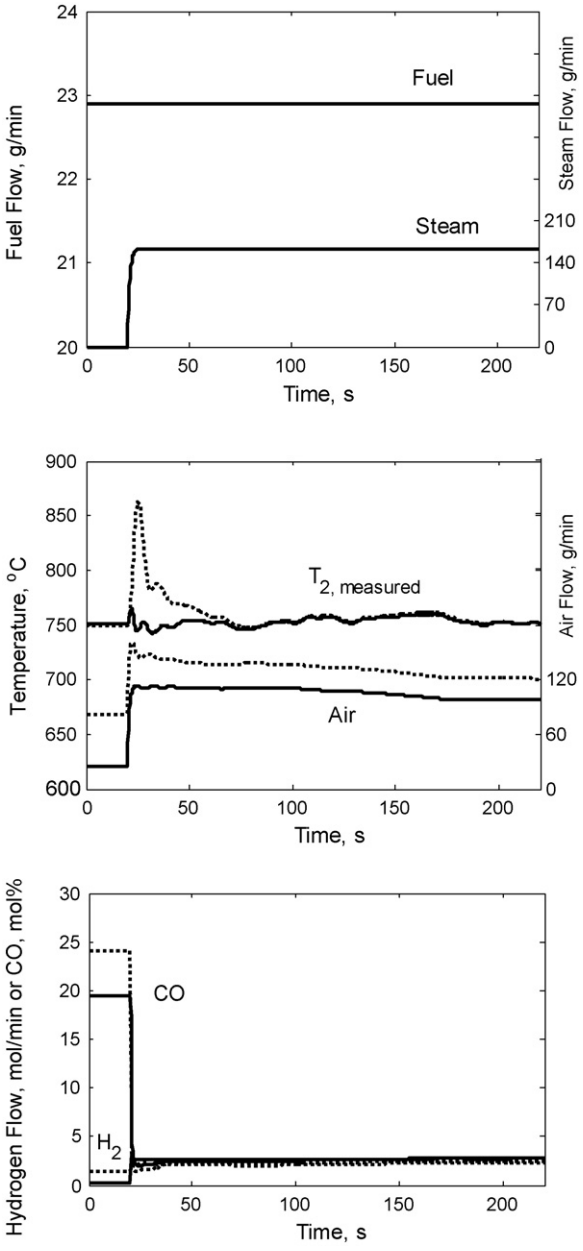

Fig. 14. Input and output responses to start-up with feed-forward control for different gasolines (solid line: $C_{7.3}H_{14.28}$; dotted line: C_8H_{18}).

rate and injecting steam to the reactor. Additionally, the start-up scenario faces the rise in inlet air temperature depicted in Fig. 8. Although this plot is just the step response output of a system with transfer function $425/(150s+1)(50s+1)(25s+1)$, its behavior is similar to the experimentally observed warm up of the heat exchanger shown in Fig. 2 [2]. Unfortunately, due to the large discrepancy between the models of the two modes (compare the parameters of Tables 2 and 3) it is unclear as to which model should be used in the controller design. As a compromise, we used the average of the two: $K_2 = 5.0$, $\tau_2 = 6.8$ and $\theta_2 = 4.3$.

As shown in Fig. 9, the feedback controller allows for an unacceptable drop in reactor temperature (~200 °C) and would extinguish the reactor for this fast steam injection case (see the solid lines). Slowing the steam injection will reduce the temperature dip to 100 °C as shown in Fig. 9 (see dotted lines). This temperature dip is expected to be enough to again extinguish the reaction. This poor performance is expected due to the larger time delay ($\theta_2 = 4.3$) of the manipulated channel as compared with that of the steam flow disturbance channel ($\theta_2 = 2.3$, the average of the values from Tables 2 and 3). Hence, feedback control alone is not expected to meet the performance objectives required for start-up.

5. Feed-forward control

Although the feedback structure of the previous section will respond to slow load changes, it is postulated that a feed-forward element will allow for faster load changes as well as meet the start-up objectives. The feed-forward plus feedback structure used in this section is depicted in Fig. 10.

The feedback controllers are identical to those of Section 4. The feed-forward element is added between the measured disturbance (steam flow rate) and the MV (air flow rate). This feed-forward element has the following lead–lag transfer function:

$$G_{ff}(s) = K_f \frac{\tau_1 s + 1}{\tau_2 s + 1} \quad (6)$$

where K_f is the static gain which is tuned to eliminate the static offset of the system; τ_1 and τ_2 are time constants which are adjusted to acquire the best dynamic performance based on the detailed tuning procedure described in [13].

5.1. Feed-forward control during nominal operation

As discussed in Section 4.1, the feedback controller responded poorly to a large load change, initiated by changes in steam and fuel flow rates. Fig. 11 compares the responses of the system with the feed-forward element for various steam and fuel injection rates. If the hydrogen demand is changed from 3 to 6 mol min^{-1}, with the feed-forward element in place (in this case, $K_f = 0.51$, $\tau_1 = 2.0$ s and $\tau_2 = 1.9$ s), we clearly see a significant improvement in performance. For both fast and slow injections, the temperature is well controlled to within ±10 °C for the whole time horizon. However, for the slow injection, the hydrogen yield will respond slowly (around 150 s), similar to that observed in Section 4.1.

5.2. Feed-forward control during start-up

With the feed-forward element and fast steam injection ($\tau_s = 1$ s), the control system works very well (see the solid lines of Fig. 12). The temperature is well controlled to within ±10 °C and the hydrogen yield and CO concentration respond quickly (around 3 s). It is noted that, due to the large discrepancy between CPOX mode and ATR mode, the parameters of the feed-forward element were changed from those used in Section 5.1 ($K_f = 0.53$, $\tau_1 = 2.0$ s and $\tau_2 = 1.6$ s). However, poor performance may be observed when the steam injection rate is reduced, e.g., $\tau_s = 3$ s (see the dotted lines of Fig. 12). With the same feed-forward controller, the reactor temperature will drop past the lower bound of 700 °C and may extinguish the reaction. Retuning the feed-forward parameters is one of the option to improve performance.

5.3. Model mismatch for feed-forward control

The results presented above demonstrate a significant improvement in performance when feed-forward control is employed. However due to the complexity of the gasoline fuel, a variation of composition is expected. To see if the feed-forward controller can handle this type of model mismatch we modified the fuel from $C_{7.3}H_{14.28}$ to *n*-octane C_8H_{18}. The heat capacity of the fuel and heats of combustion and reforming were accordingly changed. However, other parameters such as reaction rates, viscosity and thermal conductivity were unchanged.

Fig. 13 compares the performance of the feed-forward controller with and without model mismatch for a large load change during ATR operation (same scenario as Fig. 11, $\tau_s = 1$ s). As evidenced by the large initial dip in temperature, performance is significantly degraded. In Fig. 14 we see that similar poor performance is observed during the start-up scenario. The initial jump in reactor temperature (up to 850 °C) may damage the catalyst and will decrease hydrogen yield.

6. Conclusions

In this work, we proposed a feed-forward plus feedback control structure aimed at regulating the temperature of an ATR reactor. In particular, it was found that a classic control scheme is capable of sufficient disturbance attenuation under the assumption of a fixed operating condition. However, during large load changes and the CPOX to ATR mode transition associated with start-up, we found that the feedback only configuration is expected to yield poor performance (mainly due to the large time delay associated with plant dynamics). Additionally, it was found that feed-forward control could be used to improve performance during these difficult to control scenarios. It should, however, be noted that the feed-forward controller was quite sensitive to model mismatch and disturbance characteristics (as evidenced by Figs. 13, 14 and 12, respectively). This suggests that performance improvements may be possible by the development of a model-based predictive controller, which is capable of incorporating both parameter estimate data as well as disturbance characteristics. The challenge will be to achieve a reactor model with sufficient fidelity while being fast enough for on-line implementation.

Acknowledgements

This work was supported by the U.S. Department of Energy, Hydrogen, Fuel Cells, and Infrastructure Technologies Program. Special thanks to Nancy Garland, Valri Lightner, Patrick Davis, and Steve Chalk for supporting this study. The authors also wish to thank the participants of the Feasibility of Acceptable Start-Time Experimental Reformer (FASTER) project. This was a collaborative project with contributions from Los Alamos National Laboratory, Oak Ridge National Laboratory, Pacific Northwest National Laboratory, and a number of universities and private organizations providing catalysts, heat exchangers, and hardware build support. The authors gratefully acknowledge the team at Argonne National Laboratory who participated in the assembly, tests, hardware design, and analysis of the fuel processor: Steven Calderone, Tod Harvey, Shel-

don Lee, Hsui-Kai Liao, Daniel Applegate, Vincent Novick, Rajesh Ahluwalia, Steven Lottes, and Shabbir Ahmed.

References

[1] S. Ahmed, R. Ahluwalia, S.H.D. Lee, S. Lottes, J. Power Sources 9 (2006) 214.
[2] D. Papadias, S.H.D. Lee, D. Chmielewski, Ind. Eng. Chem. Res. 45 (2006) 5841.
[3] S. Springmann, M. Bohnet, A. Docter, A. Lamm, G. Eigenberger, J. Power Sources 128 (2004) 13.
[4] M. Pacheco, S. Jorge, J. Kopasz, Appl. Catal. A: Gen. 250 (2003) 161.
[5] M.Y. El-Sharkh, A. Rahman, M.S. Alam, P.C. Byrne, A.A. Sakla, T. Thomas, J. Power Sources 138 (2004) 199.
[6] H. Gorgun, M. Arcak, S. Varigonda, S.A. Bortoff, Proceedings of the 2004 American Control Conference, 2004, p. 845.
[7] J.T. Pukrushpan, A.G. Stefanopoulou, S. Varigonda, L.M. Pedersen, S. Ghosh, H. Peng, IEEE Trans. Cont. Syst. Technol. 13 (2005) 3.
[8] J. Pukrushpan, A. Stefanopoulou, S. Varigonda, J. Eborn, C. Haugstetter, in: Proceedings of the IFAC Symposium on Advances Automotive System 2004, Salerno, IFAC Cont. Eng. Prac. 14 (2006) 277.
[9] S. Varigonda, J. Pukrushpan, A.G. Stefanopoulou, Proceedings of the Fuel Cell Topical Conference at the 2003 AIChE Spring Meeting, 2003, p. 101.
[10] K. Kiryu, US Patent 6,565,817 (2003).
[11] S.D. Burch, S.G. Goebel, W.H. Pettit, US Patent 6,805,721 (2004).
[12] Y. Hu, D.J. Chmielewski, D. Papadias, Ind. Eng. Chem. Res., (2008), in press.
[13] D.E. Seborg, T.F. Edgar, D.A. Mellichamp, Process Dynamics and Control, 2nd ed., John Wiley & Sons, Hoboken, NJ, 2004.